

## Electronic Supplementary Information

### Palladium(II) and palladium(II)-silver(I) complexes of N-heterocyclic carbene and zwitterionic thiolate mixed ligands: synthesis, structural characterization and catalytic properties

Yu-Ting Wang,<sup>a</sup> Bin-Bin Gao,<sup>a</sup> Fan Wang,<sup>a</sup> Shi-Yuan Liu,<sup>a</sup> Hong Yu,<sup>\*a</sup> Wen-Hua Zhang<sup>\*a</sup> and Jian-Ping Lang<sup>\*ab</sup>

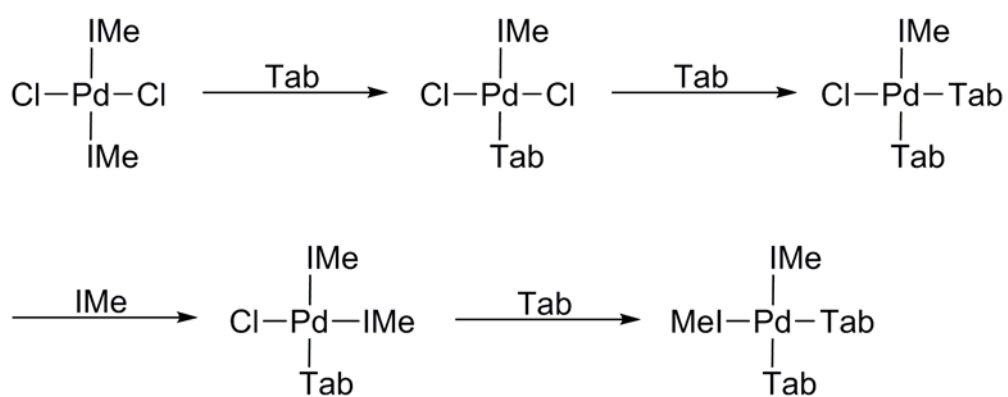
<sup>a</sup> College of Chemistry, Chemical Engineering and Materials Science, Soochow University, Suzhou 215123, Jiangsu, P. R. China

<sup>b</sup> State Key Laboratory of Organometallic Chemistry, Shanghai Institute of Organic Chemistry, Chinese Academy of Sciences, Shanghai 200032, P. R. China

## Table of Contents

<b>Scheme S1</b> Proposed reaction sequence for <b>3a</b> , <b>3b</b> and <b>4</b> .....	S4
<b>Table S1</b> Selected bond lengths ( $\text{\AA}$ ) and angles ( $^\circ$ ) for <b>2–6</b> .....	S5
<b>Fig. S1</b> (a) The positive-ion ESI mass spectrum (black) and the calculated isotope pattern (gray) of the $[\text{Pd}(\text{IMe})_2(\text{Tab})_2(\text{OTf})]^+$ cation of <b>2</b> . (b) The positive-ion ESI mass spectrum (black) and the calculated isotope pattern (gray) of the $[\text{Pd}(\text{IMe})(\text{Tab})_2(\text{OH}\cdot\text{Et}_2\text{O}\cdot\text{MeOH}\cdot\text{H}_2\text{O})]^+$ cation of <b>2</b> . (c) The positive-ion ESI mass spectrum (black) and the calculated isotope pattern (gray) of the $[\text{Pd}(\text{IMe})_2(\text{Tab})(\text{OH}\cdot 3\text{MeOH})]^+$ cation of <b>2</b> .....	S8
<b>Fig. S2</b> (a) The positive-ion ESI mass spectrum (black) and the calculated isotope pattern (gray) of the $[\text{Pd}_2(\text{IMe})_4(\text{Tab})_2(\text{PF}_6)]^{3+}$ trication of <b>4</b> . (b) The positive-ion ESI mass spectrum (black) and the calculated isotope pattern (gray) of the $[\text{Pd}_2(\text{IMe})_3(\text{Tab})_2(\text{PF}_6)_3]^+$ cation of <b>4</b> . (c) The positive-ion ESI mass spectrum (black) and the calculated isotope pattern (gray) of the $[\text{Pd}(\text{IMe})_2(\text{Tab})_2(\text{PF}_6)]^+$ cation of <b>4</b> . (d) The positive-ion ESI mass spectrum (black) and the calculated isotope pattern (gray) of the $[\text{Pd}(\text{IMe})(\text{Tab})_2]^{2+}$ dication of <b>4</b> . (e) The positive-ion ESI mass spectrum (black) and the calculated isotope pattern (gray) of the $[\text{Pd}(\text{IMe})(\text{Tab})(\text{PF}_6)\cdot 2\text{MeOH}]^+$ cation of <b>4</b> .....	S9
<b>Fig. S3</b> (a) The positive-ion ESI mass spectrum (black) and the calculated isotope pattern (gray) of the $[\text{Pd}_2(\text{IMe})_2(\text{Tab})_4(\text{OTf})_2]^{2+}$ dication of <b>5</b> . (b) The positive-ion ESI mass spectrum (black) and the calculated isotope pattern (gray) of the $[\text{Pd}_2(\text{IMe})_2(\text{Tab})_3(\text{OTf})_2]^{2+}$ dication of <b>5</b> . (c) The positive-ion ESI mass spectrum (black) and the calculated isotope pattern (gray) of the $[\text{Pd}(\text{IMe})(\text{Tab})\cdot 4\text{MeOH}\cdot 2\text{H}_2\text{O}]^{2+}$ dication after removal of <b>5</b> . (d) The positive-ion ESI mass spectrum (black) and the calculated isotope pattern (gray) of the $[\text{Ag}(\text{IMe})_2\cdot \text{MeOH}\cdot 4\text{H}_2\text{O}]^+$ cation after removal of <b>5</b> .....	S10
<b>Fig. S4</b> (a) The positive-ion ESI mass spectrum (black) and the calculated isotope pattern (gray) of the $[\text{Pd}(\text{IMe})_2(\text{Tab})_2]^{2+}$ dication of <b>6</b> . (b) The positive-ion ESI mass spectrum (black) and the calculated isotope pattern (gray) of the $[\text{Pd}(\text{IMe})(\text{Tab})\cdot 3\text{MeOH}]^{2+}$ dication of <b>6</b> . (c) The positive-ion ESI mass spectrum (black) and the calculated isotope pattern (gray) of the $[\text{Pd}(\text{IMe})(\text{Tab})(\text{PF}_6)\cdot 2\text{MeOH}]^+$ cation of <b>6</b> . (d) The positive-ion ESI mass spectrum (black) and the calculated isotope pattern (gray) of the $[\text{Pd}(\text{IMe})(\text{OH})\cdot 2\text{MeOH}]^+$ cation after removal of <b>6</b> . (e) The	

positive-ion ESI mass spectrum (black) and the calculated isotope pattern (gray) of the $[\text{Ag}(\text{IMe})_2 \cdot 2\text{H}_2\text{O}]^+$ cation after removal of <b>6</b> . (f) The positive-ion ESI mass spectrum (black) and the calculated isotope pattern (gray) of the $[\text{Ag}(\text{IMe}) \cdot 2\text{H}_2\text{O}]^+$ cation after removal of <b>6</b> .....S11
NMR spectra for the catalytic products.....S12
NMR spectra for <b>2</b> , <b>4</b> , <b>5</b> and <b>6</b> .....S21



**Scheme S1** Proposed reaction sequence for **3a**, **3b** and **4**.

**Table S1** Selected bond lengths (Å) and angles (°) for **2–6**.

Compound <b>2</b>			
Pd(1)-C(1)#1	2.0205(14)	Pd(1)-S(1)	2.3266(4)
Pd(1)-C(1)	2.0206(14)	Pd(1)-S(1)#1	2.3267(4)
C(1)#1-Pd(1)-C(1)	180.00(9)	C(1)#1-Pd(1)-S(1)#1	88.07(4)
C(1)#1-Pd(1)-S(1)	91.93(4)	C(1)-Pd(1)-S(1)#1	91.93(4)
C(1)-Pd(1)-S(1)	88.07(4)	S(1)-Pd(1)-S(1)#1	180.00(2)
#1 -x, -y + 2, -z + 1			
Compound <b>3a</b>			
Pd(1)-C(24)	2.026(4)	Pd(1)-S(2)	2.3379(12)
Pd(1)-C(19)	2.023(14)	Pd(1)-S(1)	2.3587(12)
Pd(1)-C(19A)	2.031(12)		
C(24)-Pd(1)-C(19)	89.4(9)	C(24)-Pd(1)-S(1)	178.49(13)
C(24)-Pd(1)-C(19A)	92.8(8)	C(19)-Pd(1)-S(1)	89.3(8)
C(24)-Pd(1)-S(2)	92.49(12)	C(19A)-Pd(1)-S(1)	85.8(8)
C(19)-Pd(1)-S(2)	176.3(7)	S(2)-Pd(1)-S(1)	88.90(4)
C(19A)-Pd(1)-S(2)	169.2(5)		
Compound <b>3b·MeCN</b>			
Pd(1)-C(6)	2.007(3)	Pd(1)-S(1)	2.3392(8)
Pd(1)-C(1)	2.012(3)	Pd(1)-S(2)	2.3668(8)
C(6)-Pd(1)-C(1)	89.22(13)	C(6)-Pd(1)-S(2)	91.71(9)
C(6)-Pd(1)-S(1)	174.53(9)	C(1)-Pd(1)-S(2)	179.06(10)
C(1)-Pd(1)-S(1)	96.03(9)	S(1)-Pd(1)-S(2)	83.04(3)
Compound <b>4·2MeCN</b>			
Pd(1)-C(10)	2.020(3)	Pd(1)-S(1)	2.3784(7)
Pd(1)-C(15)	2.026(3)	S(1)-Pd(1)#1	2.3767(6)
Pd(1)-S(1)#1	2.3768(6)		
C(10)-Pd(1)-C(15)	89.07(10)	C(15)-Pd(1)-S(1)	91.80(7)
C(10)-Pd(1)-S(1)#1	92.70(7)	S(1)#1-Pd(1)-S(1)	86.36(2)
C(15)-Pd(1)-S(1)#1	177.23(7)	Pd(1)#1-S(1)-Pd(1)	93.64(2)
C(10)-Pd(1)-S(1)	177.86(8)		
#1 -x, -y + 1, -z			

Compound 5

Pd(1)-C(1)	1.995(11)	Pd(2)-C(6)	2.023(10)
Pd(1)-S(2)	2.324(2)	Pd(2)-S(2)	2.326(2)
Pd(1)-S(3)#1	2.347(2)	Pd(2)-S(3)	2.341(2)
Pd(1)-S(1)	2.383(3)	Pd(2)-S(1)	2.388(2)
Pd(1)···Pd(2)	3.1289(9)	S(3)-Pd(1)#1	2.347(2)
C(1)-Pd(1)-S(2)	93.1(3)	S(2)-Pd(2)-S(3)	167.65(10)
C(1)-Pd(1)-S(3)#1	90.8(3)	C(6)-Pd(2)-S(1)	174.1(3)
S(2)-Pd(1)-S(3)#1	171.19(9)	S(2)-Pd(2)-S(1)	80.25(8)
C(1)-Pd(1)-S(1)	172.7(3)	S(3)-Pd(2)-S(1)	89.59(8)
S(2)-Pd(1)-S(1)	80.38(8)	C(6)-Pd(2)-Pd(1)	125.3(3)
S(3)#1-Pd(1)-S(1)	95.21(8)	S(2)-Pd(2)-Pd(1)	47.68(6)
C(1)-Pd(1)-Pd(2)	123.8(3)	S(3)-Pd(2)-Pd(1)	128.46(6)
S(2)-Pd(1)-Pd(2)	47.74(6)	S(1)-Pd(2)-Pd(1)	48.96(6)
S(3)#1-Pd(1)-Pd(2)	123.86(6)	Pd(1)-S(1)-Pd(2)	81.96(8)
S(1)-Pd(1)-Pd(2)	49.08(6)	Pd(1)-S(2)-Pd(2)	84.58(8)
C(6)-Pd(2)-S(2)	94.4(3)	Pd(2)-S(3)-Pd(1)#1	105.61(9)
C(6)-Pd(2)-S(3)	96.0(3)		
#1 $-x, -y, -z + 1$			

---

**Compound 6**

Ag(1)-S(3)	2.4536(18)	Pd(1)-C(1)	1.98(2)
Ag(1)-S(1)	2.5351(18)	Pd(1)-C(6)	2.011(6)
Ag(1)-S(2)	2.6875(17)	Pd(1)-C(1A)	2.033(13)
Ag(1)-S(4)#1	2.7404(15)	Pd(1)-S(1)	2.3613(16)
Ag(1)…Pd(1)	3.2482(9)	Pd(1)-S(2)	2.3841(17)
Ag(2)-S(3)	2.4834(16)	Pd(2)-C(56)	2.016(6)
Ag(2)-S(4)	2.5057(16)	Pd(2)-C(61)	2.022(6)
Ag(2)-S(5)#1	2.5618(17)	Pd(2)-S(4)	2.3620(15)
Ag(2)…Ag(2)#1	3.0004(10)	Pd(2)-S(5)	2.3731(15)
S(3)-Ag(1)-S(1)	144.61(6)	C(6)-Pd(1)-S(2)	176.96(17)
S(3)-Ag(1)-S(2)	121.74(5)	C(1A)-Pd(1)-S(2)	92.3(7)
S(1)-Ag(1)-S(2)	76.69(5)	S(1)-Pd(1)-S(2)	86.19(5)
S(3)-Ag(1)-S(4)#1	101.93(5)	C(1)-Pd(1)-Ag(1)	133.5(13)
S(1)-Ag(1)-S(4)#1	99.66(5)	C(6)-Pd(1)-Ag(1)	122.59(17)
S(2)-Ag(1)-S(4)#1	107.77(5)	C(1A)-Pd(1)-Ag(1)	131.6(7)
S(3)-Ag(1)-Pd(1)	122.50(4)	S(1)-Pd(1)-Ag(1)	50.78(5)
S(1)-Ag(1)-Pd(1)	46.19(4)	S(2)-Pd(1)-Ag(1)	54.42(4)
S(2)-Ag(1)-Pd(1)	46.18(4)	C(56)-Pd(2)-C(61)	91.1(2)
S(4)#1-Ag(1)-Pd(1)	135.32(4)	C(56)-Pd(2)-S(4)	174.26(18)
S(3)-Ag(2)-S(4)	134.28(6)	C(61)-Pd(2)-S(4)	94.38(17)
S(3)-Ag(2)-S(5)#1	110.24(5)	C(56)-Pd(2)-S(5)	89.90(17)
S(4)-Ag(2)-S(5)#1	115.06(5)	C(61)-Pd(2)-S(5)	174.62(18)
S(3)-Ag(2)-Ag(2)#1	118.32(4)	S(4)-Pd(2)-S(5)	84.74(5)
S(4)-Ag(2)-Ag(2)#1	76.45(4)	Pd(1)-S(1)-Ag(1)	83.04(5)
S(5)#1-Ag(2)-Ag(2)#1	79.89(4)	Pd(1)-S(2)-Ag(1)	79.40(5)
C(1)-Pd(1)-C(6)	94.6(13)	Ag(1)-S(3)-Ag(2)	93.05(6)
C(6)-Pd(1)-C(1A)	90.4(7)	Pd(2)-S(4)-Ag(2)	88.28(5)
C(1)-Pd(1)-S(1)	165.6(7)	Pd(2)-S(4)-Ag(1)#1	109.67(5)
C(6)-Pd(1)-S(1)	91.24(17)	Ag(2)-S(4)-Ag(1)#1	125.44(6)
C(1A)-Pd(1)-S(1)	174.8(5)	Pd(2)-S(5)-Ag(2)#1	116.29(6)
C(1)-Pd(1)-S(2)	88.3(13)		

#1 -x + 3/2, -y + 3/2, -z + 1

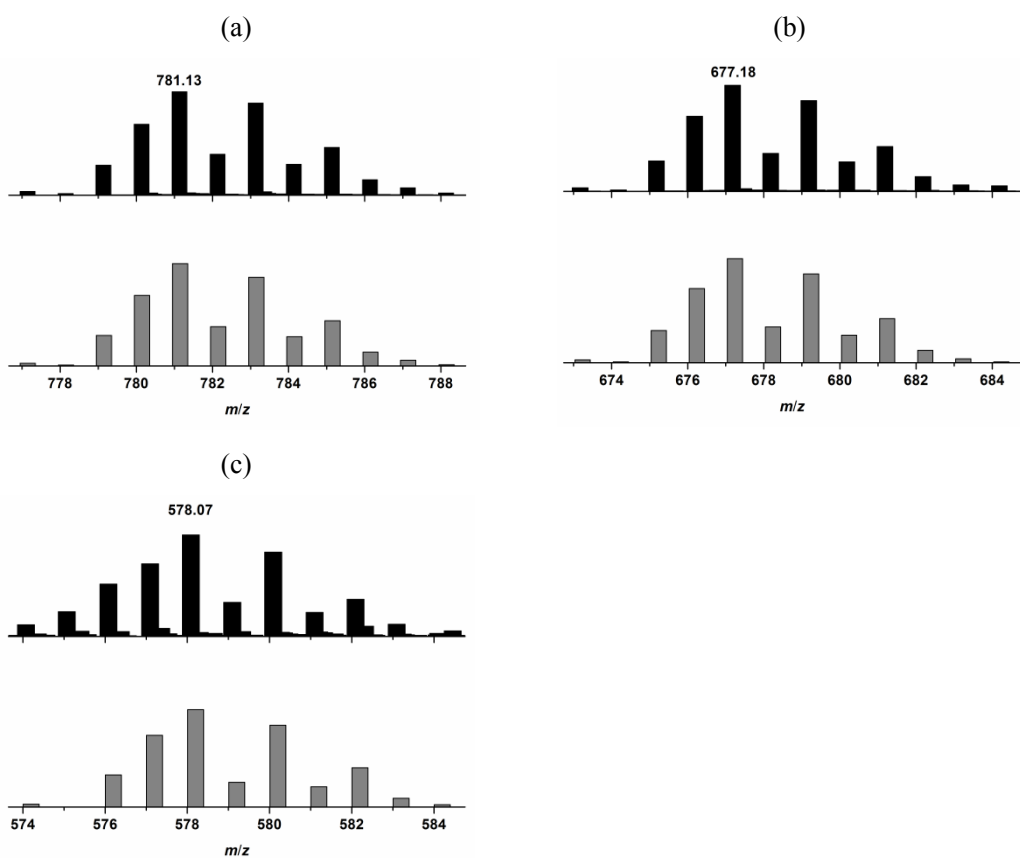


**Fig. S1** (a) The positive-ion ESI mass spectrum (black) and the calculated isotope pattern (gray) of the  $[\text{Pd}(\text{IMe})_2(\text{Tab})_2(\text{OTf})]^+$  cation of **2**. (b) The positive-ion ESI mass spectrum (black) and the calculated isotope pattern (gray) of the  $[\text{Pd}(\text{IMe})(\text{Tab})_2(\text{OH}) \cdot \text{Et}_2\text{O} \cdot \text{MeOH} \cdot \text{H}_2\text{O}]^+$  cation of **2**. (c) The positive-ion ESI mass spectrum (black) and the calculated isotope pattern (gray) of the  $[\text{Pd}(\text{IMe})_2(\text{Tab})(\text{OH}) \cdot 3\text{MeOH}]^+$  cation of **2**.

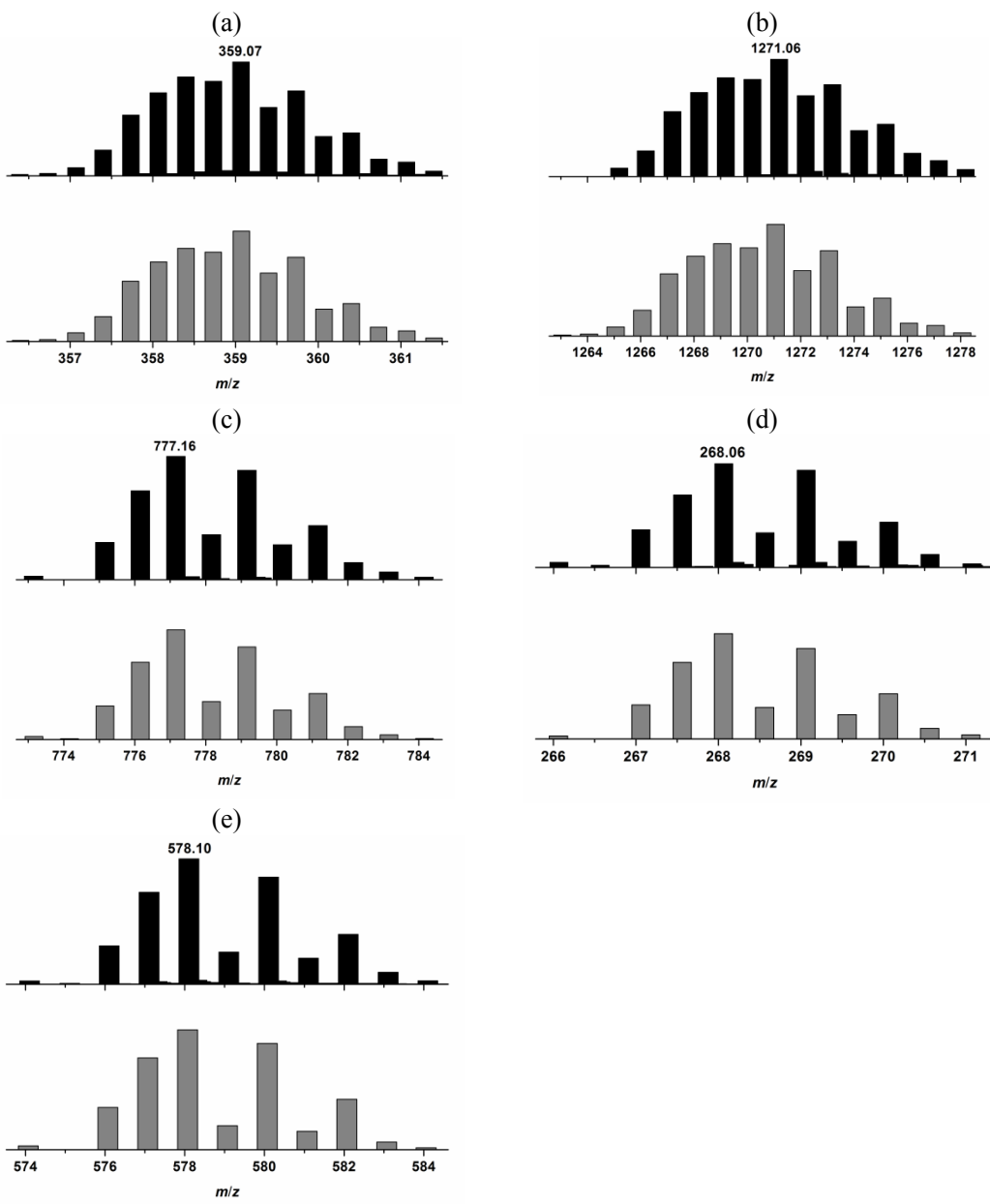


**Fig. S2** (a) The positive-ion ESI mass spectrum (black) and the calculated isotope pattern (gray) of the  $[\text{Pd}_2(\text{IMe})_4(\text{Tab})_2(\text{PF}_6)]^{3+}$  trication of **4**. (b) The positive-ion ESI mass spectrum (black) and the calculated isotope pattern (gray) of the  $[\text{Pd}_2(\text{IMe})_3(\text{Tab})_2(\text{PF}_6)_3]^{+}$  cation of **4**. (c) The positive-ion ESI mass spectrum (black) and the calculated isotope pattern (gray) of the  $[\text{Pd}(\text{IMe})_2(\text{Tab})_2(\text{PF}_6)]^{+}$  cation of **4**. (d) The positive-ion ESI mass spectrum (black) and the calculated isotope pattern (gray) of the  $[\text{Pd}(\text{IMe})(\text{Tab})_2]^{2+}$  dication of **4**. (e) The positive-ion ESI mass spectrum (black) and the calculated isotope pattern (gray) of the  $[\text{Pd}(\text{IMe})(\text{Tab})(\text{PF}_6) \cdot 2\text{MeOH}]^{+}$  cation of **4**.

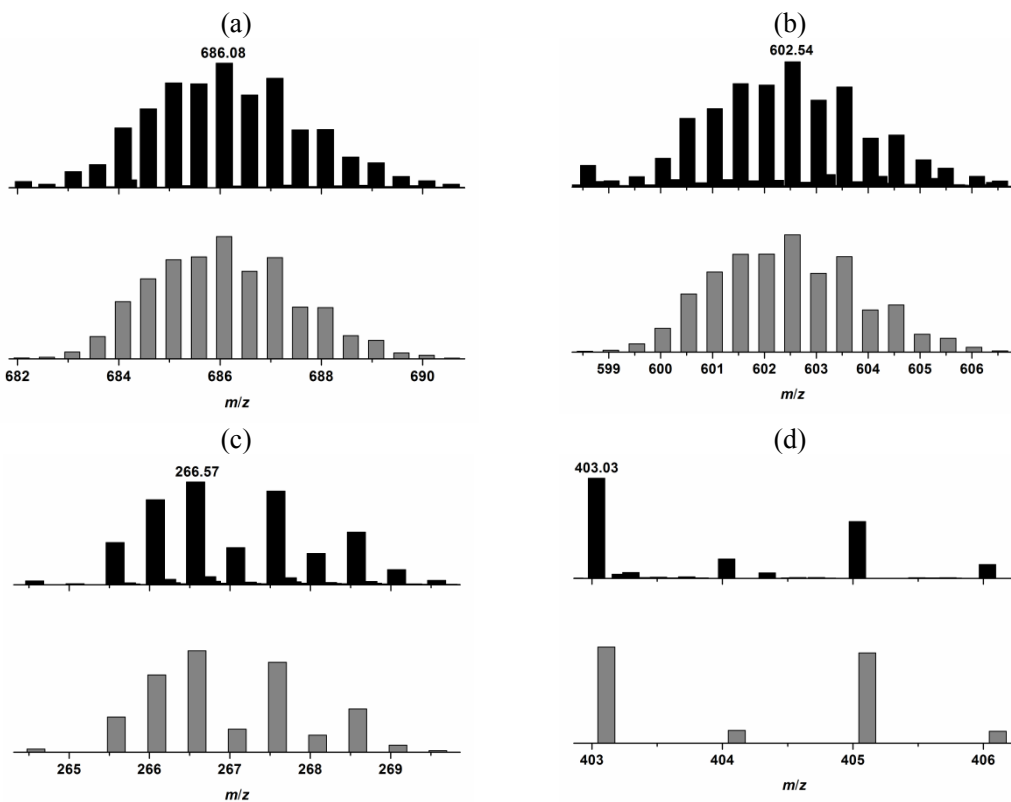


**Fig. S3** (a) The positive-ion ESI mass spectrum (black) and the calculated isotope pattern (gray) of the  $[\text{Pd}_2(\text{IMe})_2(\text{Tab})_4(\text{OTf})_2]^{2+}$  dication of **5**. (b) The positive-ion ESI mass spectrum (black) and the calculated isotope pattern (gray) of the  $[\text{Pd}_2(\text{IMe})_2(\text{Tab})_3(\text{OTf})_2]^{2+}$  dication of **5**. (c) The positive-ion ESI mass spectrum (black) and the calculated isotope pattern (gray) of the  $[\text{Pd}(\text{IMe})(\text{Tab}) \cdot 4\text{MeOH} \cdot 2\text{H}_2\text{O}]^{2+}$  dication after removal of **5**. (d) The positive-ion ESI mass spectrum (black) and the calculated isotope pattern (gray) of the  $[\text{Ag}(\text{IMe})_2 \cdot \text{MeOH} \cdot 4\text{H}_2\text{O}]^+$  cation after removal of **5**.

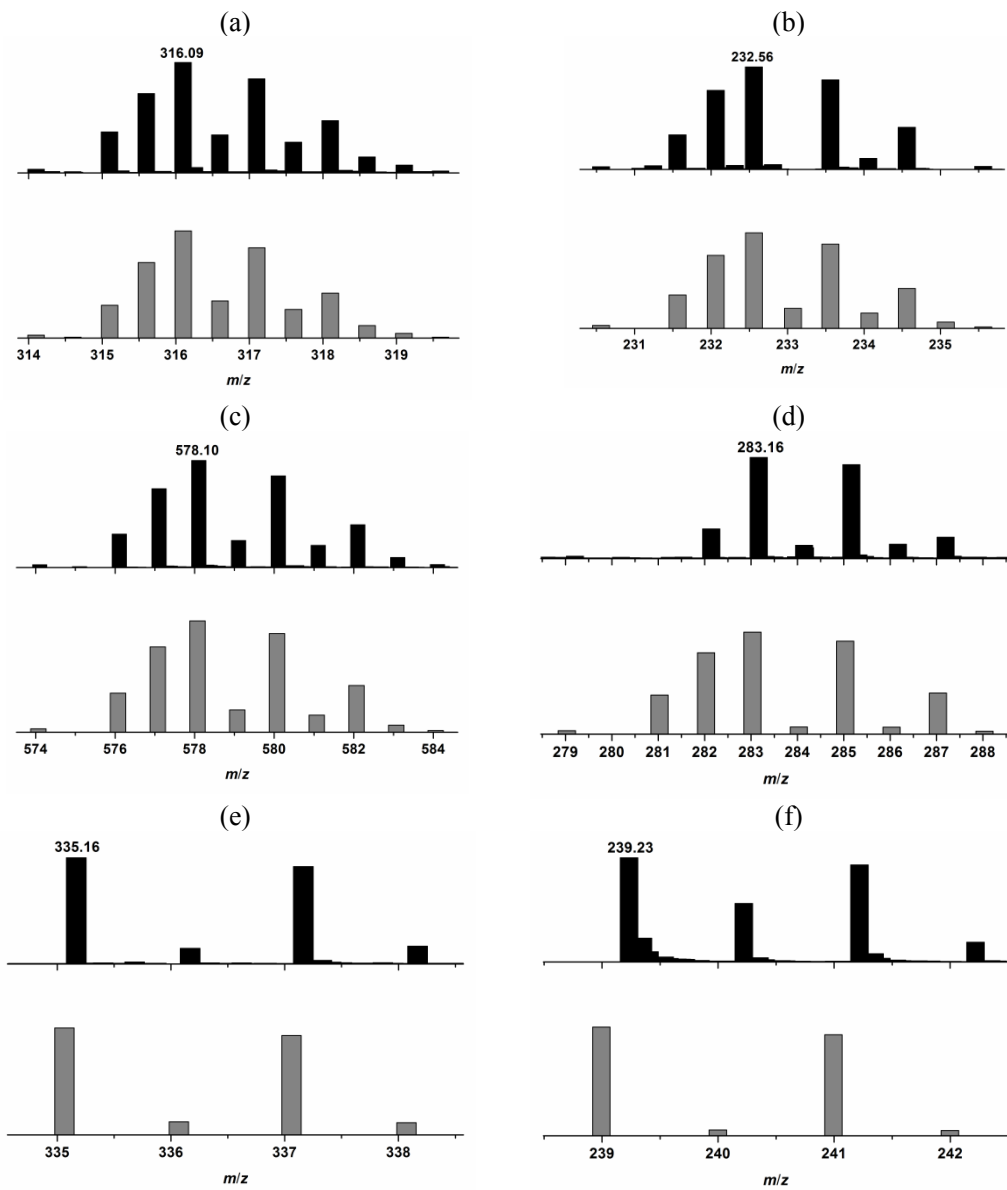
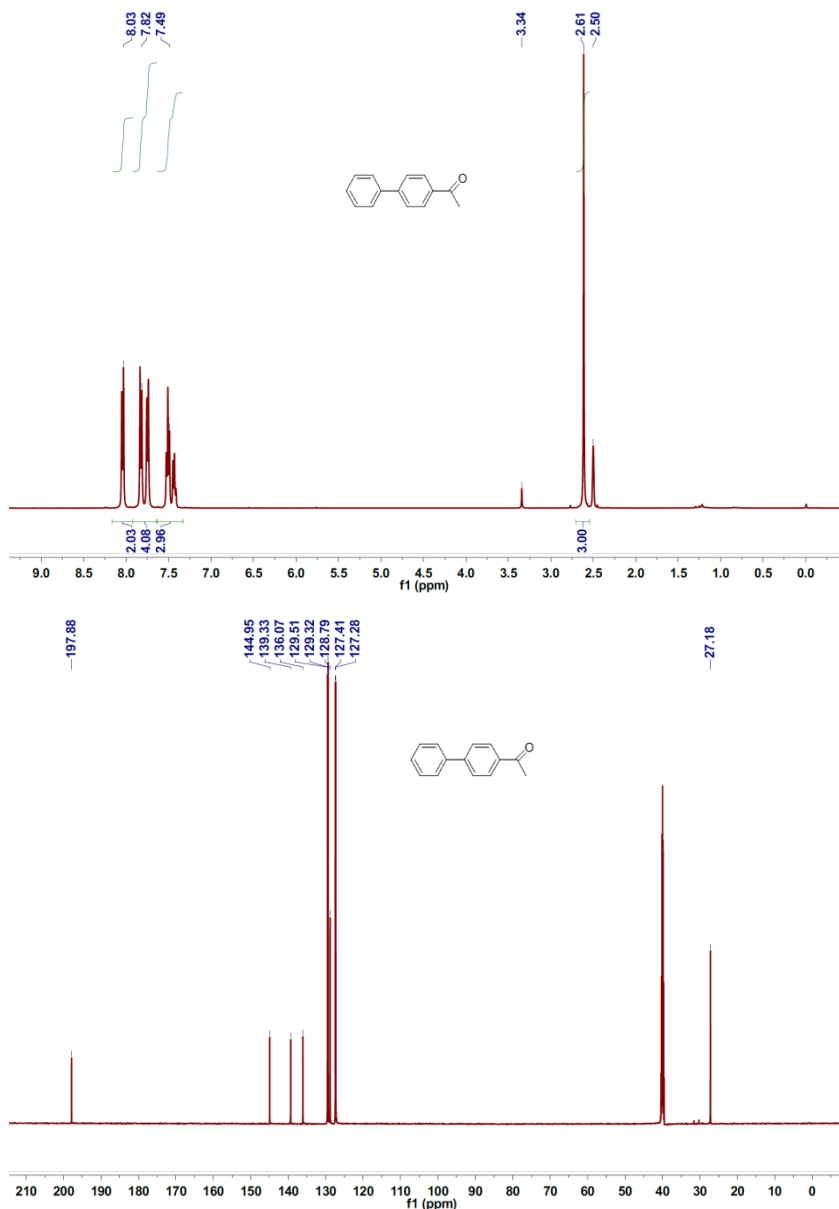
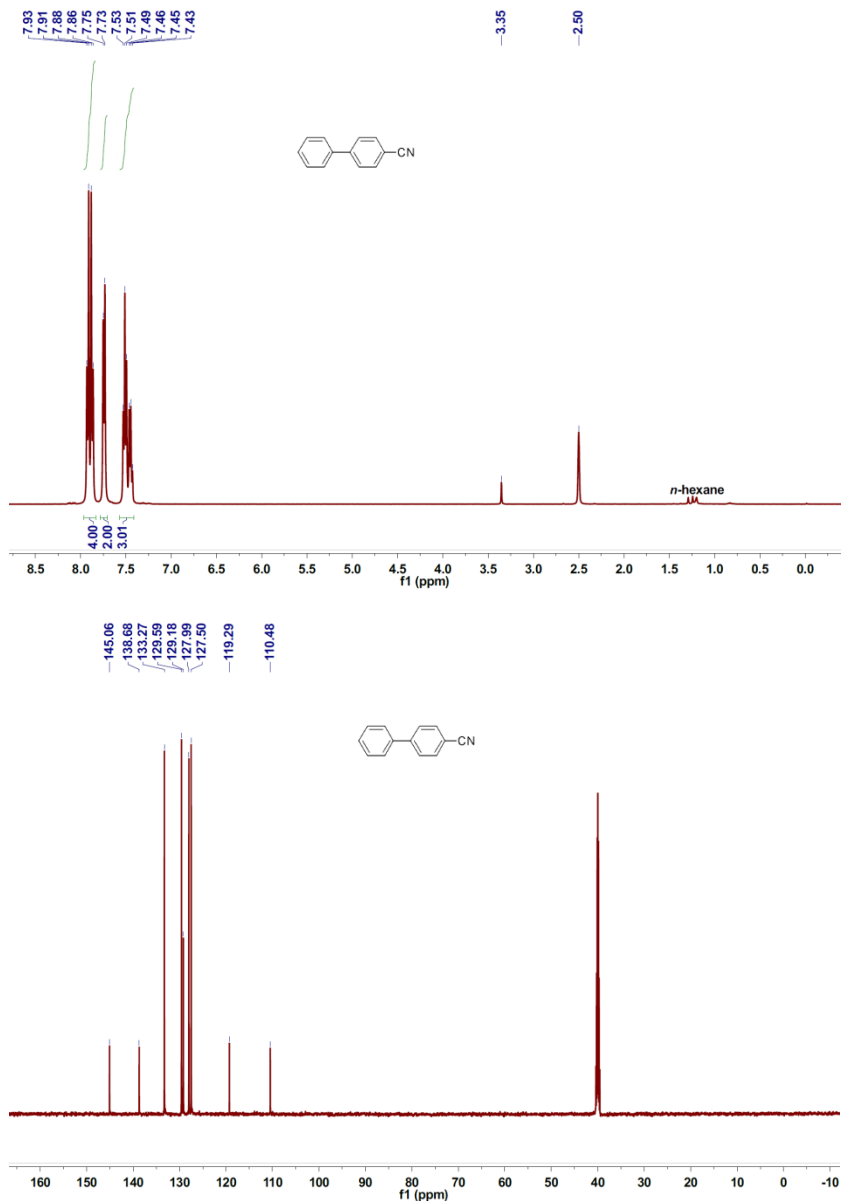


**Fig. S4** (a) The positive-ion ESI mass spectrum (black) and the calculated isotope pattern (gray) of the  $[\text{Pd}(\text{IMe})_2(\text{Tab})_2]^{2+}$  dication of **6**. (b) The positive-ion ESI mass spectrum (black) and the calculated isotope pattern (gray) of the  $[\text{Pd}(\text{IMe})(\text{Tab}) \cdot 3\text{MeOH}]^{2+}$  dication of **6**. (c) The positive-ion ESI mass spectrum (black) and the calculated isotope pattern (gray) of the  $[\text{Pd}(\text{IMe})(\text{Tab})(\text{PF}_6) \cdot 2\text{MeOH}]^+$  cation of **6**. (d) The positive-ion ESI mass spectrum (black) and the calculated isotope pattern (gray) of the  $[\text{Pd}(\text{IMe})(\text{OH}) \cdot 2\text{MeOH}]^+$  cation after removal of **6**. (e) The positive-ion ESI mass spectrum (black) and the calculated isotope pattern (gray) of the  $[\text{Ag}(\text{IMe})_2 \cdot 2\text{H}_2\text{O}]^+$  cation after removal of **6**. (f) The positive-ion ESI mass spectrum (black) and the calculated isotope pattern (gray) of the  $[\text{Ag}(\text{IMe}) \cdot 2\text{H}_2\text{O}]^+$  cation after removal of **6**.

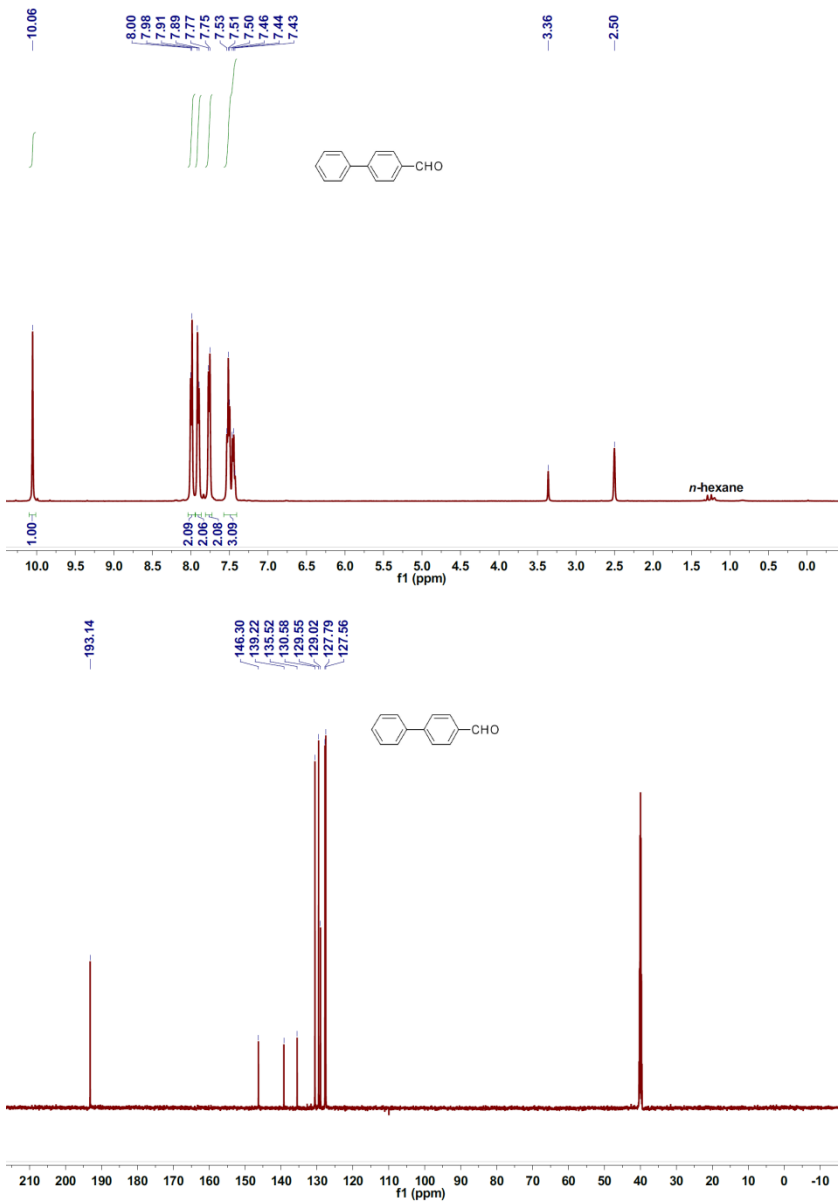
NMR spectra for the catalytic products



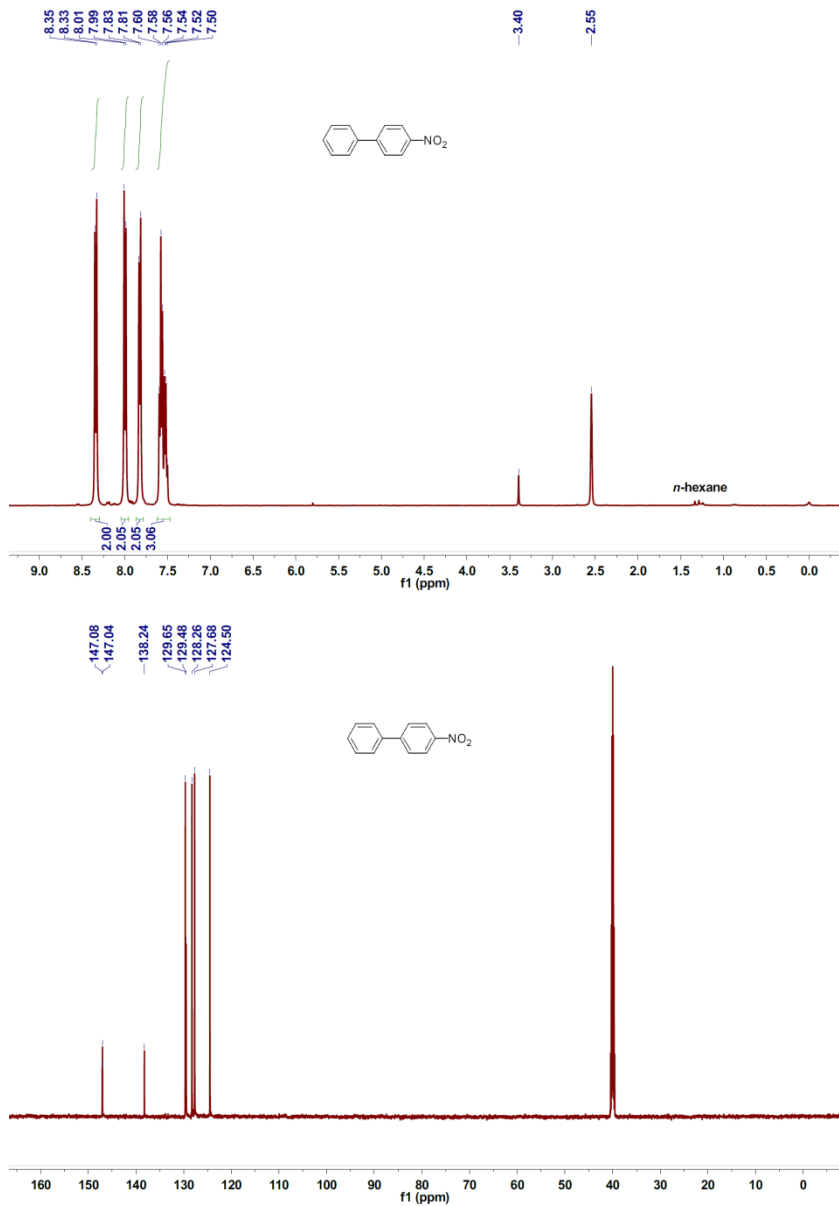
**4-acetyl-biphenyl (1).**  $^1\text{H}$  NMR (400 MHz,  $\text{DMSO}-d_6$ , ppm):  $\delta$  8.03 (s, 2H), 7.83 (d,  $J = 8.1$  Hz, 2H), 7.75 (d,  $J = 7.5$  Hz, 2H), 7.51 (t,  $J = 7.4$  Hz, 2H), 7.43 (t,  $J = 7.2$  Hz, 1H), 2.61 (s, 3H);  $^{13}\text{C}$  NMR (101 MHz,  $\text{DMSO}-d_6$ , ppm):  $\delta$  197.88 (s), 144.95 (s), 139.33 (s), 136.07 (s), 129.51 (s), 129.32 (s), 128.79 (s), 127.41 (s), 127.28 (s), 27.18 (s).



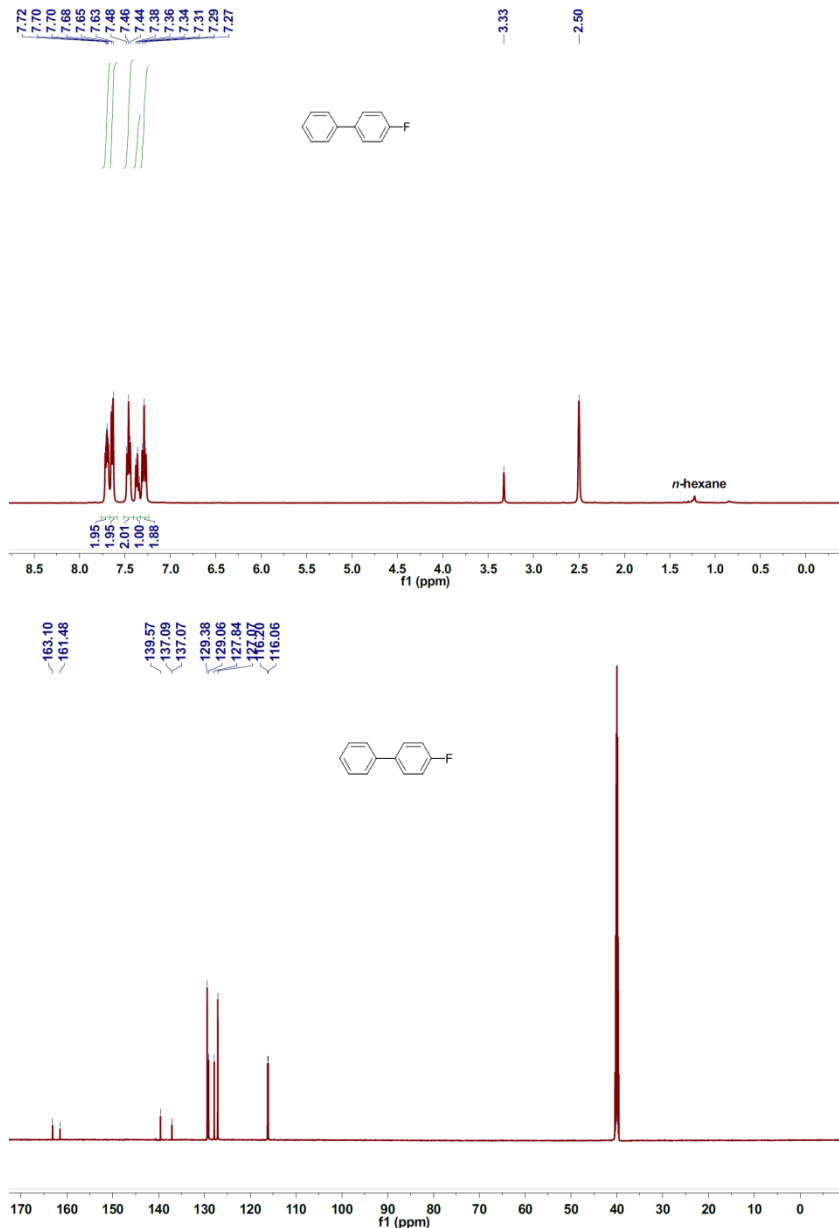
**4-carbonitrile-biphenyl (2).**  $^1\text{H}$  NMR (400 MHz, DMSO- $d_6$ , ppm):  $\delta$  7.90 (dd,  $J$  = 19.5, 8.2 Hz, 4H), 7.74 (d,  $J$  = 7.5 Hz, 2H), 7.48 (dt,  $J$  = 26.0, 7.2 Hz, 3H);  $^{13}\text{C}$  NMR (101 MHz, DMSO- $d_6$ , ppm):  $\delta$  145.06 (s), 138.68 (s), 133.27 (s), 129.59 (s), 129.18 (s), 127.99 (s), 127.50 (s), 119.29 (s), 110.48 (s).



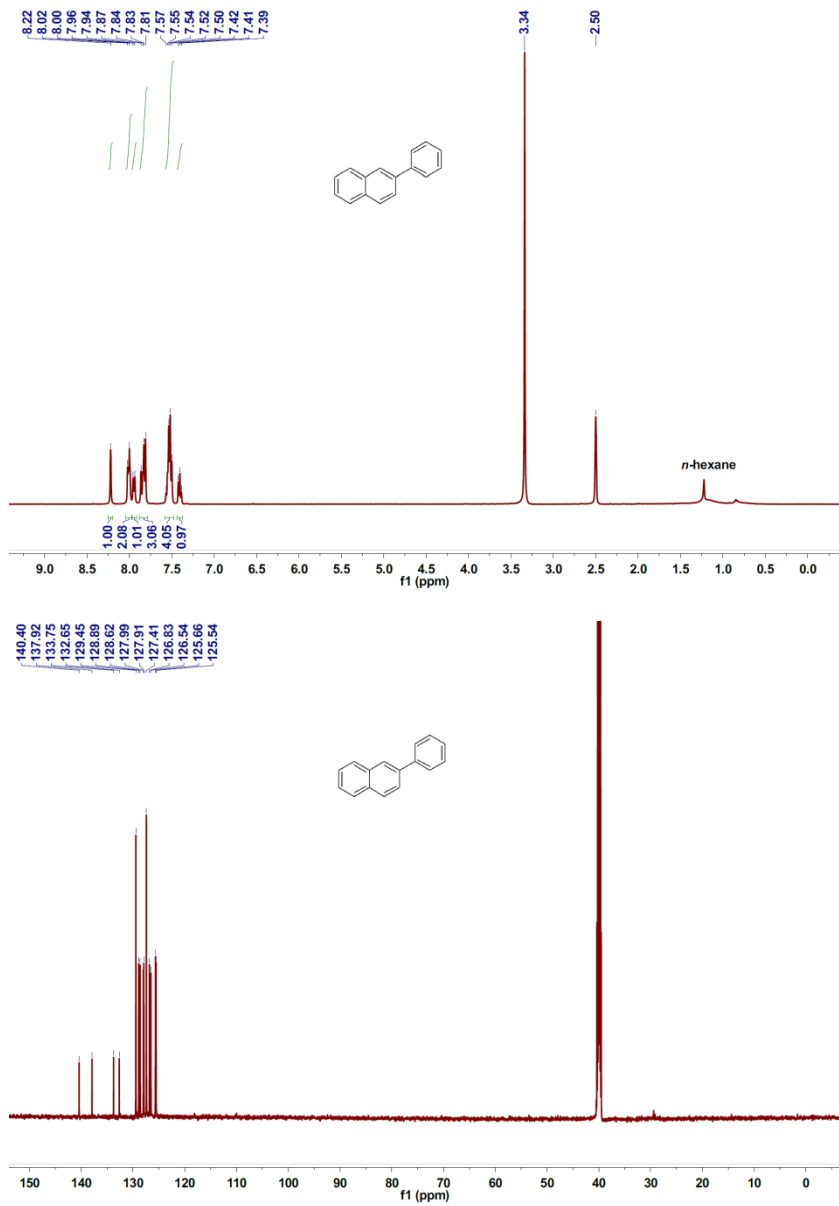
**4-carbaldehyde-biphenyl (3).**  $^1\text{H}$  NMR (400 MHz, DMSO-*d*<sub>6</sub>, ppm):  $\delta$  10.06 (s, 1H), 7.99 (d,  $J = 7.9$  Hz, 2H), 7.90 (d,  $J = 7.8$  Hz, 2H), 7.76 (d,  $J = 7.4$  Hz, 2H), 7.48 (dt,  $J = 28.0, 7.1$  Hz, 3H);  $^{13}\text{C}$  NMR (101 MHz, DMSO-*d*<sub>6</sub>, ppm):  $\delta$  193.14 (s), 146.30 (s), 139.22 (s), 135.52 (s), 130.58 (s), 129.55 (s), 129.02 (s), 127.79 (s), 127.56 (s).



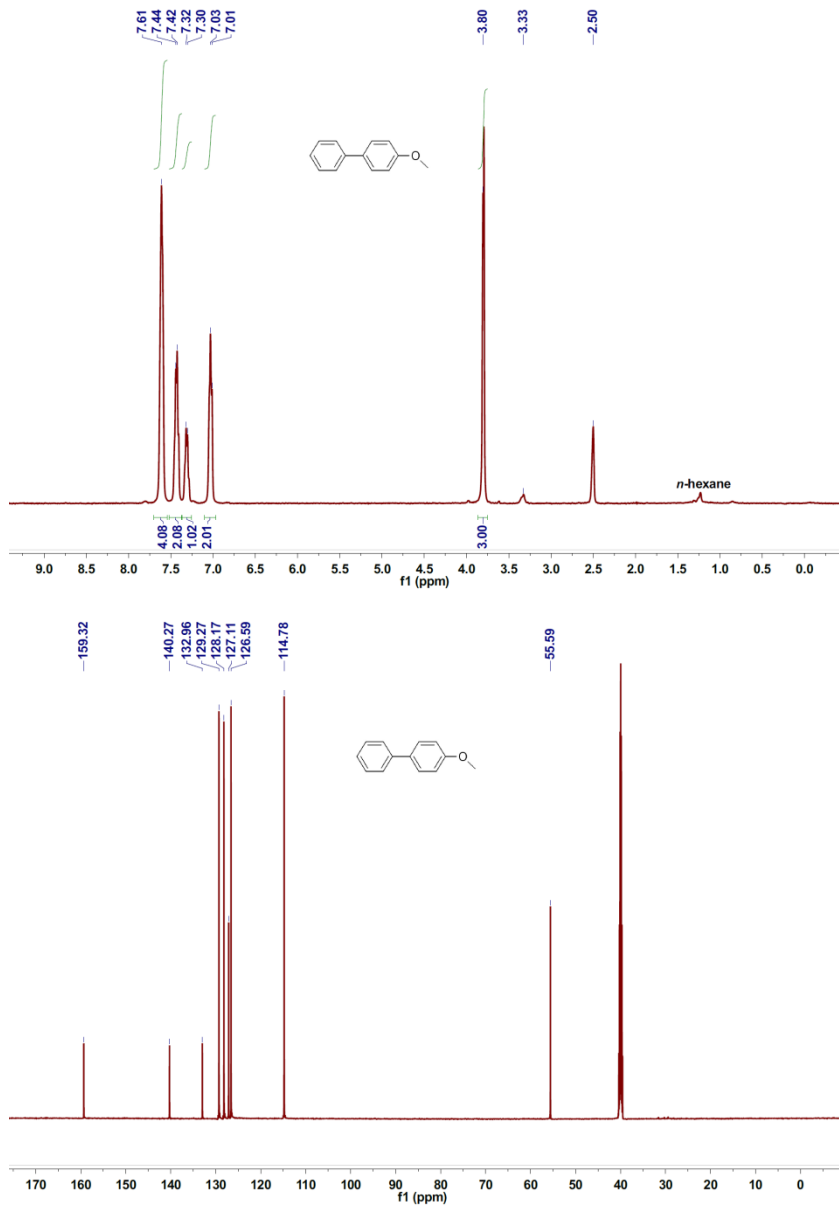
**4-nitro-biphenyl (4).**  $^1\text{H}$  NMR (400 MHz, DMSO-*d*<sub>6</sub>, ppm):  $\delta$  8.34 (d,  $J$  = 8.6 Hz, 2H), 8.00 (d,  $J$  = 8.7 Hz, 2H), 7.82 (d,  $J$  = 7.4 Hz, 2H), 7.55 (dt,  $J$  = 23.5, 7.1 Hz, 3H);  $^{13}\text{C}$  NMR (101 MHz, DMSO-*d*<sub>6</sub>, ppm):  $\delta$  147.06 (d,  $J$  = 6.5 Hz), 138.24 (s), 129.65 (s), 129.48 (s), 128.26 (s), 127.68 (s), 124.50 (s).



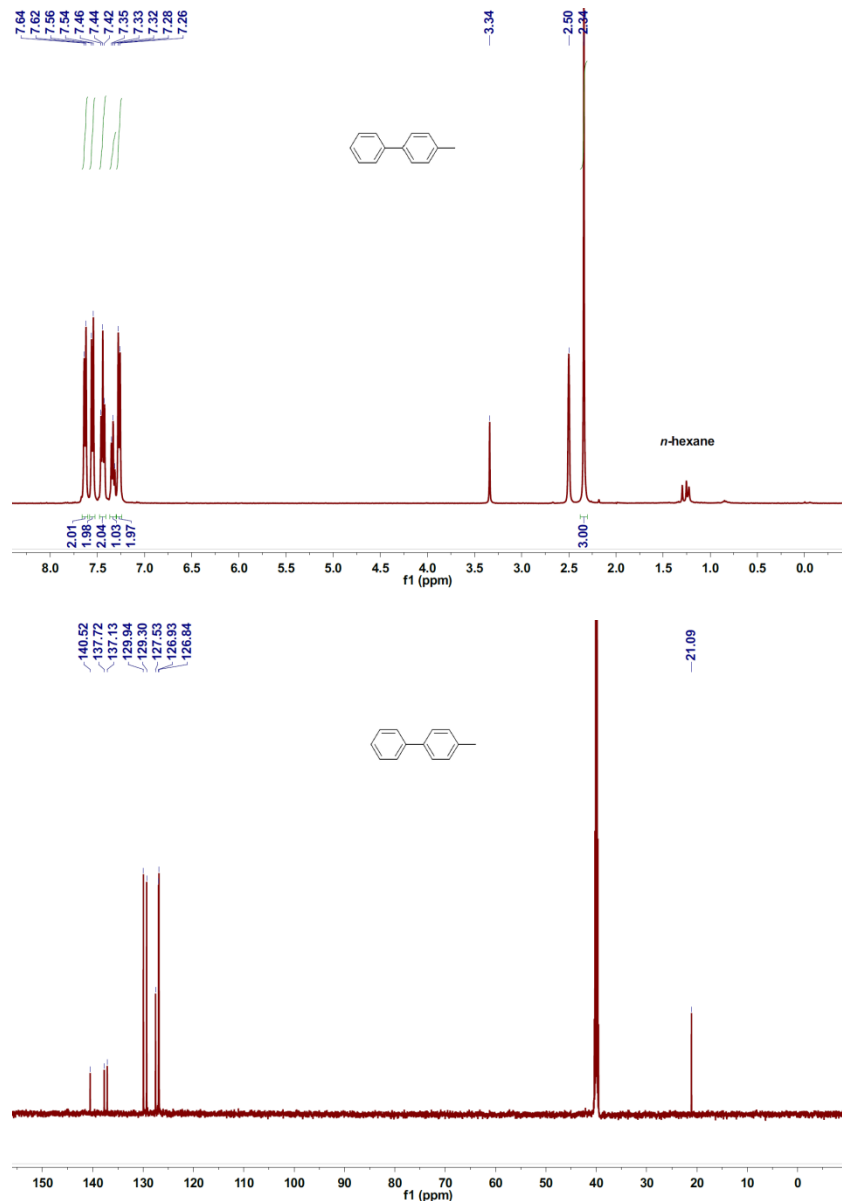
**4-fluoro-biphenyl (5).**  $^1\text{H}$  NMR (400 MHz, DMSO- $d_6$ , ppm):  $\delta$  7.70 (dd,  $J = 7.8, 6.0$  Hz, 2H), 7.64 (d,  $J = 7.5$  Hz, 2H), 7.46 (t,  $J = 7.5$  Hz, 2H), 7.36 (t,  $J = 7.3$  Hz, 1H), 7.29 (t,  $J = 8.7$  Hz, 2H);  $^{13}\text{C}$  NMR (101 MHz, DMSO- $d_6$ , ppm):  $\delta$  163.10 (s), 161.48 (s), 139.57 (s), 137.08 (d,  $J = 2.8$  Hz), 129.45-128.98 (m), 127.84 (s), 127.09 (d,  $J = 7.0$  Hz), 116.13 (d,  $J = 21.3$  Hz).



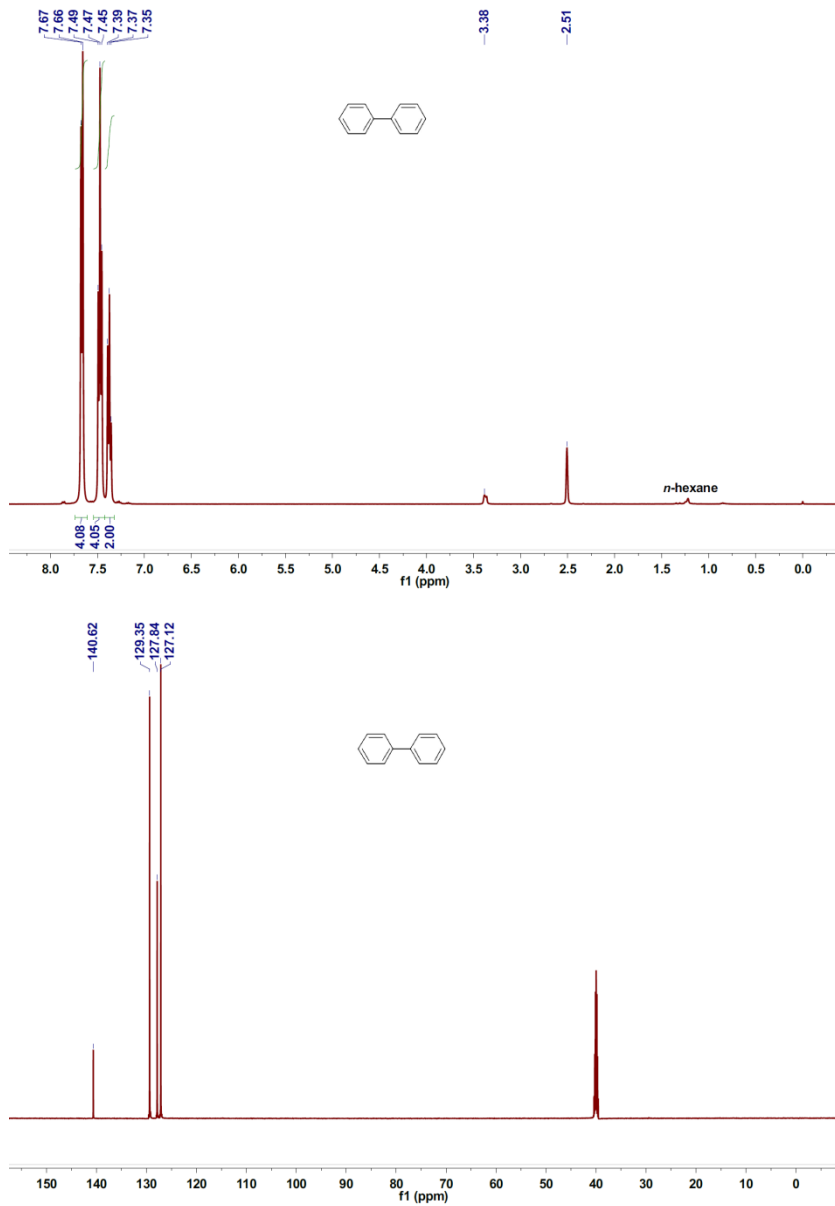
**2-phenyl-naphthalene (6).**  $^1\text{H}$  NMR (400 MHz, DMSO-*d*<sub>6</sub>, ppm):  $\delta$  8.22 (s, 1H), 8.01 (d, *J* = 8.6 Hz, 2H), 7.95 (d, *J* = 7.4 Hz, 1H), 7.88 – 7.78 (m, 3H), 7.58–7.48 (m, 4H), 7.41 (t, *J* = 7.3 Hz, 1H);  $^{13}\text{C}$  NMR (101 MHz, DMSO-*d*<sub>6</sub>, ppm):  $\delta$  140.40 (s), 137.92 (s), 133.75 (s), 132.65 (s), 129.45 (s), 128.89 (s), 128.62 (s), 127.95 (d, *J* = 12.1 Hz), 127.41 (s), 126.83 (s), 126.54 (s), 125.60 (d, *J* = 18.5 Hz).



**4-methoxybiphenyl (7).**  $^1\text{H}$  NMR (400 MHz, DMSO- $d_6$ , ppm):  $\delta$  7.61 (s, 4H), 7.43 (d,  $J = 6.1$  Hz, 2H), 7.31 (d,  $J = 6.5$  Hz, 1H), 7.02 (d,  $J = 7.4$  Hz, 2H), 3.80 (s, 3H);  $^{13}\text{C}$  NMR (101 MHz, DMSO- $d_6$ , ppm):  $\delta$  159.32 (s), 140.27 (s), 132.96 (s), 129.27 (s), 128.17 (s), 127.11 (s), 126.59 (s), 114.78 (s), 55.59 (s).

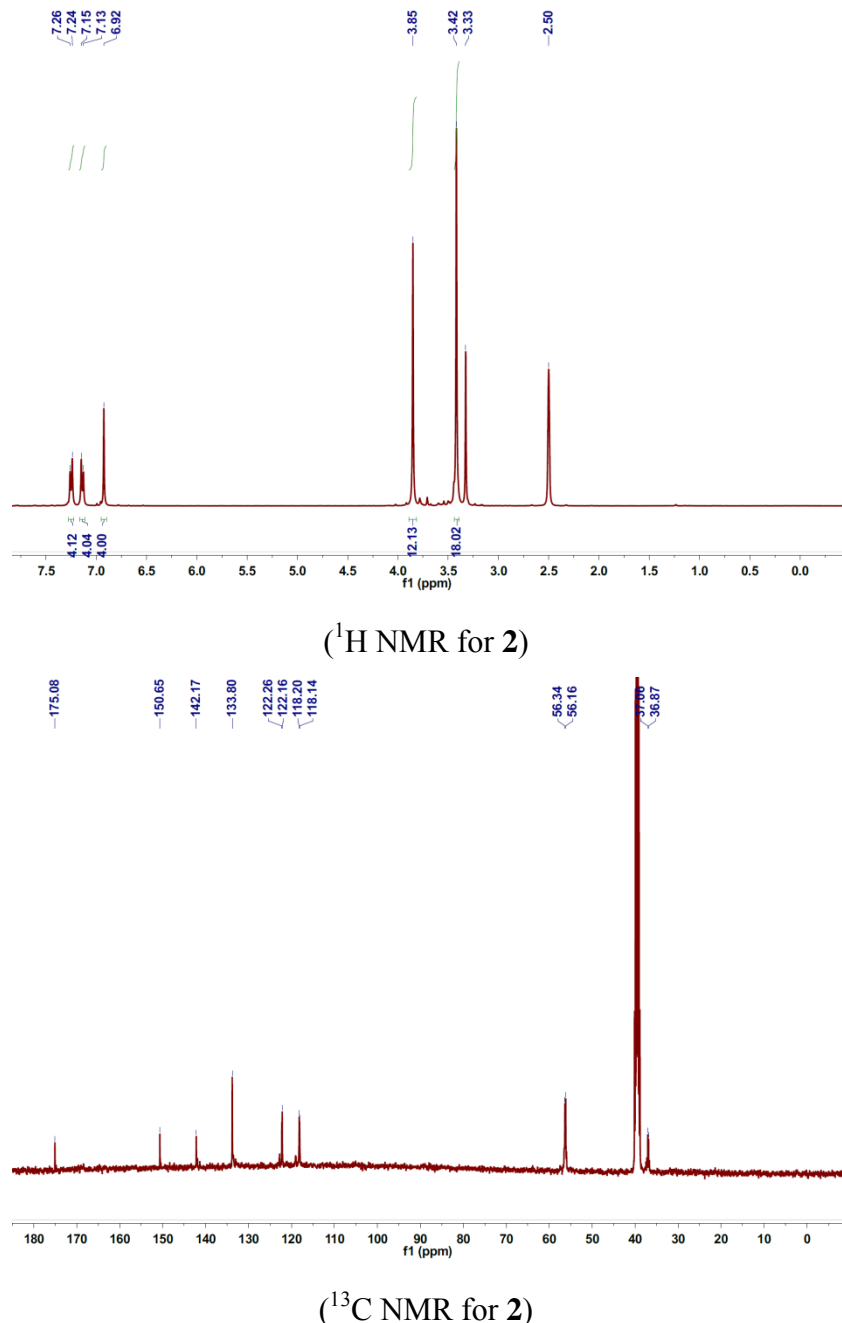


**4-methyl-biphenyl (8).**  $^1\text{H}$  NMR (400 MHz, DMSO- $d_6$ , ppm):  $\delta$  7.63 (d,  $J = 7.5$  Hz, 2H), 7.55 (d,  $J = 8.0$  Hz, 2H), 7.44 (t,  $J = 7.6$  Hz, 2H), 7.33 (t,  $J = 7.3$  Hz, 1H), 7.27 (d,  $J = 7.8$  Hz, 2H), 2.34 (s, 3H);  $^{13}\text{C}$  NMR (101 MHz, DMSO- $d_6$ , ppm):  $\delta$  140.52 (s), 137.72 (s), 137.13 (s), 129.94 (s), 129.30 (s), 127.53 (s), 126.93 (s), 126.84 (s), 21.09 (s).

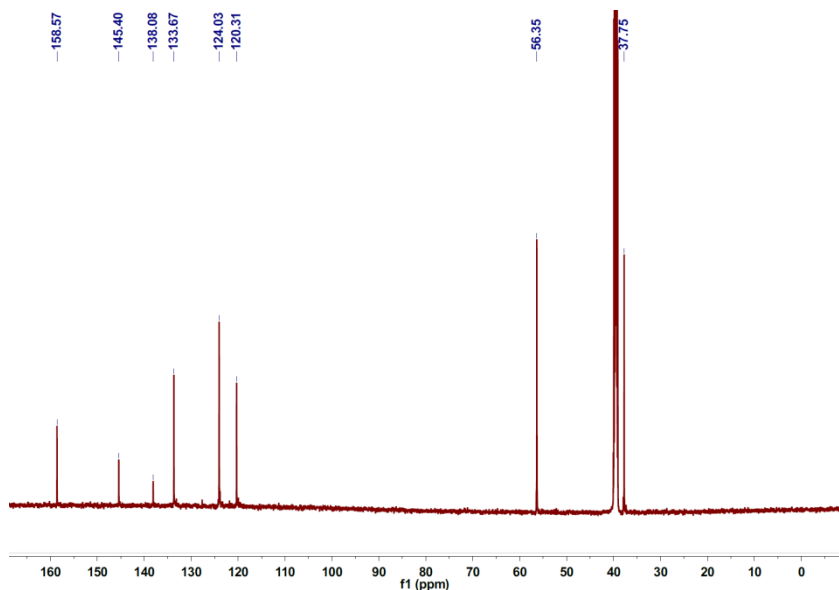
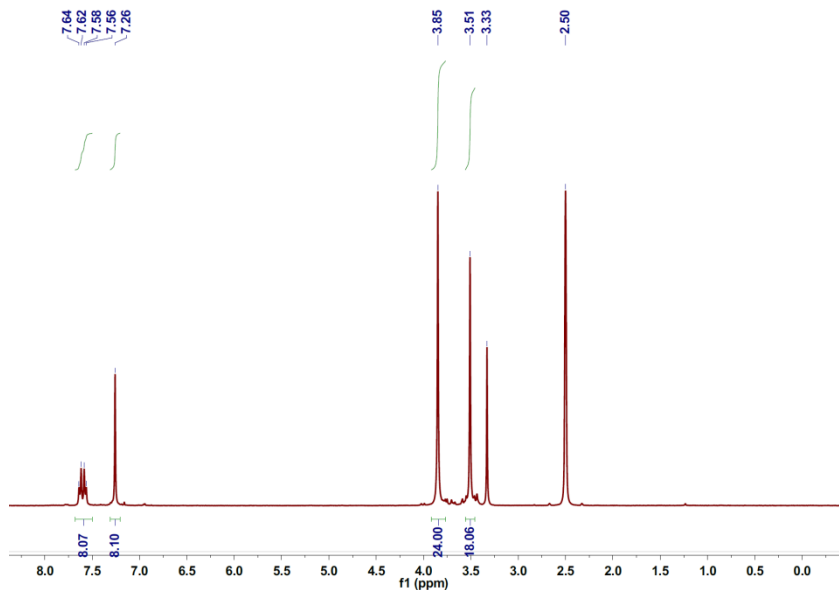


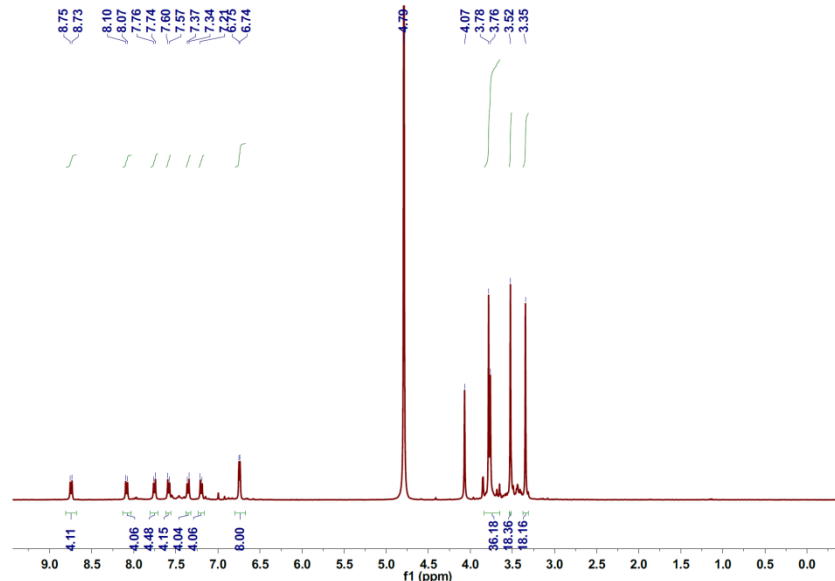
**Biphenyl (9).**  $^1\text{H}$  NMR (400 MHz, DMSO- $d_6$ , ppm):  $\delta$  7.66 (d,  $J = 7.5$  Hz, 4H), 7.47 (t,  $J = 7.5$  Hz, 4H), 7.37 (t,  $J = 7.3$  Hz, 2H);  $^{13}\text{C}$  NMR (101 MHz, DMSO- $d_6$ , ppm):  $\delta$  140.62 (s), 129.35 (s), 127.84 (s), 127.12 (s).

NMR spectra for **2**, **4**, **5** and **6**

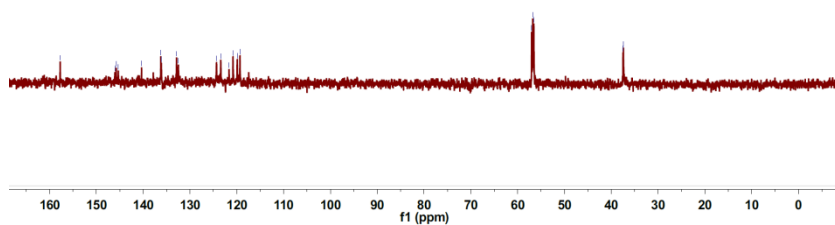


( $^1\text{H}$  NMR for **2**)





( $^1\text{H}$  NMR for **5**)



(<sup>13</sup>C NMR for **5**)

